The Astrophysical Journal, 641:L73–L76, 2006 April 10

MAGNETOCONVECTION IN A SUNSPOT UMBRA

M. Schüssler and A. Vögler[1]
Max-Planck-Institut für Sonnensystemforschung, Max-Planck-Strasse 2, D-37191 Katlenburg-Lindau, Germany;
schuessler@mps.mpg.de, voegler@mps.mpg.de
Received 2006 January 30; accepted 2006 March 1; published 2006 March 23

ABSTRACT

Results from a realistic simulation of three-dimensional radiative magnetoconvection in a strong background magnetic field corresponding to the conditions in sunspot umbrae are shown. The convective energy transport is dominated by narrow upflow plumes with adjacent downflows, which become almost field-free near the surface layers. The strong external magnetic field forces the plumes to assume a cusplike shape in their top parts, where the upflowing plasma loses its buoyancy. The resulting bright features in intensity images correspond well (in terms of brightness, size, and lifetime) to the observed umbral dots in the central parts of sunspot umbrae. Most of the simulated umbral dots have a horizontally elongated form with a central dark lane. Above the cusp, most plumes show narrow upflow jets, which are driven by the pressure of the piled-up plasma below. The large velocities and low field strengths in the plumes are effectively screened from spectroscopic observation because the surfaces of equal optical depth are locally elevated, so that spectral lines are largely formed above the cusp. Our simulations demonstrate that nearly field-free upflow plumes and umbral dots are a natural result of convection in a strong, initially monolithic magnetic field.

Subject headings: methods: numerical — MHD — Sun: magnetic fields — Sun: photosphere — sunspots

1. INTRODUCTION

Sunspot umbrae appear dark because the convective flows are suppressed by the strong magnetic field (Biermann 1941; Cowling 1953), reducing the emitted energy (per unit time and area) in the central parts of a large umbra to about 10%–20% of the average value outside sunspots. However, even this strongly diminished energy flux cannot be carried by radiation alone below the umbral photosphere (Schlüter & Temesváry 1958), so that some form of reduced convective energy transport is required in order to construct a consistent sunspot model (Deinzer 1965). The observation of umbral dots, relatively bright features of subarcsecond size embedded in the dark umbral background, has often been taken as a signature of such convective energy transport, either in the form of overstable oscillations ("elevator convection") in thin vertical columns (e.g., Savage 1969) or as intrusions from below of nonmagnetic plasma into a shallow cluster-type sunspot (Parker 1979). For monolithic sunspot models, linear stability analysis indicates that oscillatory convection in slender columns is the preferred mode in the first few thousand kilometers' depth below the umbral photosphere, where the quantity $\zeta = \eta/\kappa$, the ratio of the magnetic diffusivity η to the thermal (radiative) diffusivity κ has values smaller than unity (Meyer et al. 1974). Systematic studies based on numerical simulations under idealized conditions extend this result into the nonlinear regime (e.g., Weiss et al. 1990, 1996, 2002). Here we report on the first realistic simulations of convection in sunspot umbrae with full radiative transfer and partial ionization effects. These simulations can be compared directly with observations.

2. SIMULATION SETUP

We have carried out ab initio numerical simulations of three-dimensional radiative magnetoconvection in the near-surface layers of a sunspot umbra using the MURaM code[2] (Vögler et al. 2003; Vögler 2003;[3] Vögler et al. 2005). The computational box extends 5760 km × 5760 km in the horizontal directions and 1600 km in depth, roughly covering the range from 1200 km below to 400 km above the average level of Rosseland optical depth unity, $\tau_R = 1$. The cell size of the computational mesh is 20 km in both horizontal directions and 10 km in the vertical. We assume a constant magnetic diffusivity of 2.8×10^6 m^2 s^{-1} and hyperdiffusivities for the other diffusive processes (for details, see Vögler et al. 2005). Since here we are mainly interested in studying the convective processes around and below $\tau_R = 1$ without a detailed comparison with spectropolarimetric observations, we have included only the lower parts of the umbral atmosphere and also restricted ourselves to gray radiative transfer. The vertical magnetic flux through the box is fixed, corresponding to a horizontally averaged vertical magnetic field of 2500 G. The thermal energy density of the inflowing matter at the (open) bottom boundary has been fixed at a value of 3.5×10^{12} ergs cm^{-3}, leading to an average radiative energy output (per unit area and time) through the upper boundary around 17%–18% of its value outside sunspots.

The first phase of the thermal relaxation of the model was carried out in two dimensions for greater computational efficiency. After ~30 hours of computed solar time, we continued to evolve the model in three dimensions for ~3 hr until a statistically stationary state (i.e., no trends in energy flux and in horizontally averaged profiles of temperature and other quantities) had developed. The simulation was then continued for another 2.3 hr of solar time.

3. RESULTS

The system develops a mode of convective energy transport that is dominated by nonstationary narrow plumes of rising hot plasma. The strong expansion of the rising matter with height leads to a drastic decrease of the magnetic field strength in the upper layers of the plumes. For a snapshot from the simulation run, Figure 1 shows the brightness (vertically emerging gray intensity) together with the vertical velocity and the vertical magnetic field, the latter two at a height of $z = 1200$ km, which roughly corresponds to the average level of $\tau_R = 1$. The bright features in the intensity image have a typical size of 200–300 km, a lifetime on the order of 30 minutes, and a broad distribution of brightness values reaching up to 2.4 times the

[1] Current address: High Altitude Observatory, National Center for Atmospheric Research, P.O. Box 3000, Boulder, CO 80307.
[2] See http://www.mps.mpg.de/projects/solar-mhd/muram_site.
[3] Available at http://webdoc.sub.gwdg.de/diss/2004/voegler.

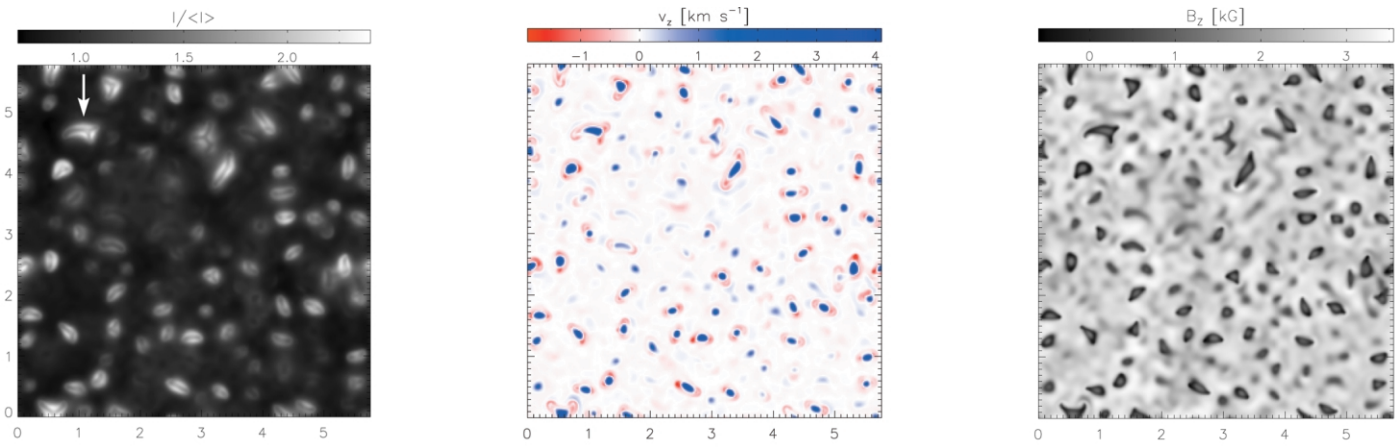

FIG. 1.—Vertically emerging gray intensity, normalized by its horizontal average (*left*), and cuts of the vertical velocity (*middle*) and vertical magnetic field (*right*) components at a height of 1200 km above the bottom of the simulation box (400 km below the top), approximately corresponding to the average level of Rosseland optical depth unity ($\tau_R = 1$), for a snapshot from the simulation run. The length unit is 1000 km. The bright features in the intensity image can be identified with umbral dots. They are caused by strong upflows in regions of significantly reduced magnetic field. The arrow indicates the umbral dot studied in more detail below.

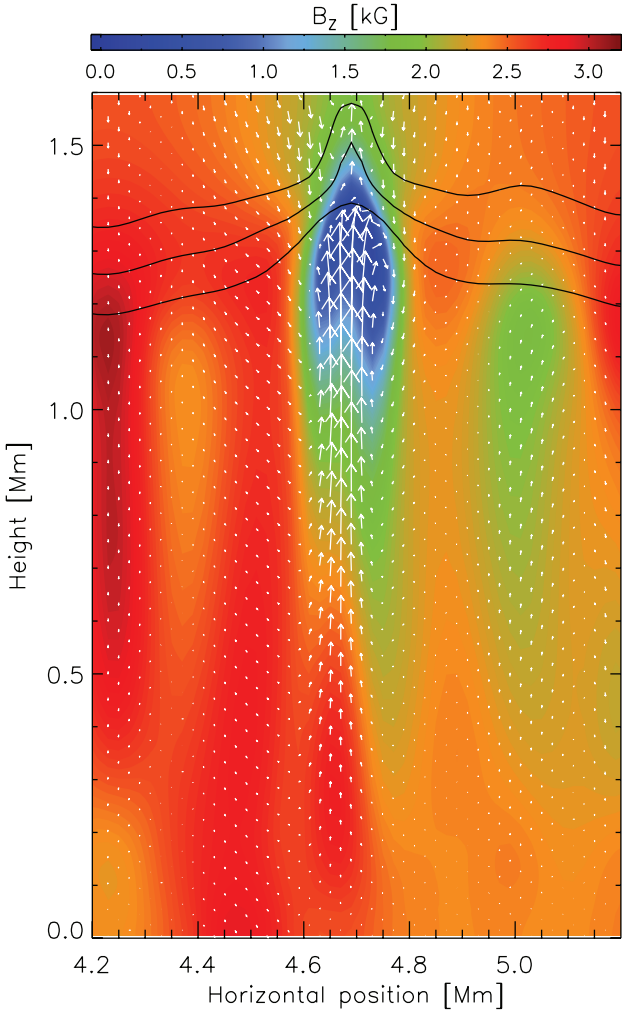

FIG. 2.—Vertical cut through the simulation box in the direction indicated by the arrow in Fig. 1, nearly perpendicular to the dark lane of the umbral dot. Colors indicate magnetic field strength, and the arrows represent (projected) velocity vectors. The longest arrow corresponds to a velocity of 2.7 km s^{-1}. The lines indicate levels of constant optical depth τ_R of 1, 0.1, and 0.01 (*bottom to top*). The upper part of the plume has developed a cusplike shape with a strongly decelerated upflow and a weak magnetic field. The flow turns horizontal mainly in the direction perpendicular to the plane of the cut.

average brightness in the simulated umbra. These values are consistent with the results of high-resolution photometry of umbral dots in the darker central parts of sunspot umbrae (Sobotka & Hanslmeier 2005). Most of the simulated umbral dots have an elongated shape with a central dark lane and downflows concentrated at the endpoints. Larger dots sometimes show a threefold dark lane with three downflow patches. These shapes may result from the fluting instability in the upper parts of the low field strength upflow channel underlying the umbral dot: the elongated features correspond to azimuthal wavenumber $m = 2$, while the threefold structure results from the mode $m = 3$.

We have studied in some detail the structure of the umbral dot indicated by the arrow in Figure 1 (*left*). A cut through the computational box in the direction of the arrow, roughly perpendicular to the dark lane, is shown in Figure 2. The cut covers the upflow plume underlying the umbral dot and its immediate environment.

The magnetic field is strongly reduced, down to values of a few hundred gauss, in the near-surface layers of the plume. The corresponding lateral expansion of the structure is mainly in the direction perpendicular to the cut shown here, leading to the elongated shape of the visible umbral dot. The upflow is strongly braked around $\tau_R = 1$, where the plasma rapidly loses its buoyancy, mainly owing to cooling by radiative losses and the mean stratification becoming subadiabatic. The plasma piles up and the flow turns horizontal (mainly in the direction perpendicular to the cut) in the region below the cusp until a quasi-stationary state with locally enhanced density and pressure is established. This is illustrated in Figure 3, which shows the density fluctuations with respect to the horizontal average at the same height in the upper central part of the cut displayed in Figure 2. As a result of the enhanced density below the cusp, the level of $\tau_R = 1$ (*solid line*) is so elevated in the central part that it cuts through regions of lower temperature (indicated by the dotted isotherms) than in the more peripheral parts. This leads to the dark lane in the intensity image; a similar mechanism has been proposed to explain the dark lanes observed in bright penumbral filaments (Spruit & Scharmer 2006). The flow turns horizontal near the surface of $\tau_R = 1$ and proceeds in the direction of the dark lane, finally descending in narrow downflow channels, which are still within the volume that the flow has largely cleared from magnetic field (cf. Fig. 1; see also Fig. 5).

An interesting feature visible in Figures 2 and 3 is a narrow jetlike upflow above the cusp. The pressure below the cusp

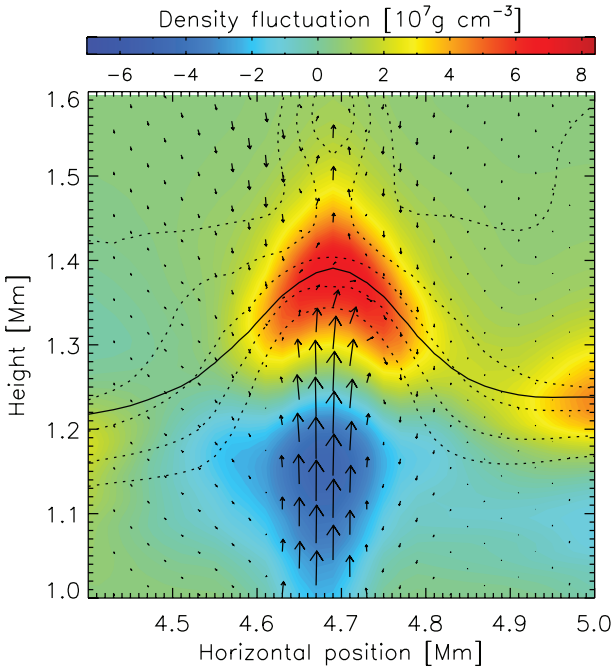

FIG. 3.—Upper central part of the cut shown in Fig. 2. Colors represent the density fluctuation with respect to the horizontal mean at the same height. The solid line indicates the level of $\tau_R = 1$, while the dotted lines are isotherms. The piling up of matter raises the surfaces of constant optical depth into low-temperature regions near the cusp, leading to the appearance of a dark lane with a maximum contrast of about 15% in the intensity image. The longest velocity arrow corresponds to a speed of 2.7 km s^{-1}.

builds up sufficiently strongly to drive matter out along the magnetic field above the cusp with a velocity of about 1 km s^{-1}, the cusp acting like a safety valve (Choudhuri 1986). Although most of the upflowing matter turns over and descends in the downflow channels and only a small part escapes upward, such outflows occur above most upflow plumes (see also Fig. 5) and could possibly affect the chromospheric dynamics above sunspots. However, since the simulation does not cover the higher layers of the umbral atmosphere and has a closed top boundary, we cannot predict the effects on the basis of the present results.

The profiles of vertical components of velocity and magnetic field along the horizontal direction of the cut shown in Figure 2 are given in Figure 4. There is a strong difference between the values inside and outside the upflow plume at constant *geometric* level, but the elevation of the lines of constant *optical* depth, together with the strong decrease of the differences with height, lead to much smaller variations in the range $\tau_R \simeq 0.01$–0.1, where most photospheric spectral lines are formed. At values $\tau_R = 0.01$ and $\tau_R = 0.1$, we find only a maximum reduction of the vertical field strength by 20% and 40%, respectively, with respect to the horizontal mean of 2500 G and maximum upflow velocities of 0.3 and 0.9 km s^{-1}. Consequently, spectroscopic observations would reveal neither the strong field reduction nor the high velocities in the upflow plumes, even if any instrumental or seeing-related smearing and stray-light effects were absent. This is consistent with existing observational results (e.g., Socas-Navarro et al. 2004).

Figure 5 shows the time evolution of a typical upflow plume developing into an umbral dot when hot plasma reaches the surface ($\tau_R = 1$). The development starts as a feeble upflow below the surface (*left*), which develops into a strong plume once the hot gas reaches the surface, cools by radiative losses, and descends in adjacent narrow downflow channels, thereby forming an overturning cell. The expanding rising plasma creates a "gap" in the magnetic field that develops into a cusplike configuration outlined by the dark lane in the brightness images. The jet- or sheetlike upflow above the cusp driven by the steeper pressure gradient of the piled-up plasma below is clearly visible in the velocity cuts. Since there is no sustained buoyancy driving from below to supply the strong upflow in the upper layers driven by radiative losses, density and pressure decrease and the magnetic field strength grows in the deeper parts, and eventually, the plume fades away.

4. DISCUSSION

Our simulations show that upflow plumes and umbral dots naturally appear in strong-field magnetoconvection with radiative transfer. The plumes start off like oscillatory convection columns below the surface but turn into narrow overturning cells driven by the strong radiative cooling around optical depth unity, which leads to descending low-entropy fluid. Even though the quantity $\zeta = \eta/\kappa$ is much smaller than unity in the upper third of our computational box,[4] this mode dominates because the overturning flow is largely confined to the gap in the magnetic field

[4] Since our numerical scheme includes a spatiotemporally varying thermal "hyperdiffusivity" (Vögler et al. 2005), the value of ζ is not readily determined in the lower part of the computational box, where κ is no longer dominated by the radiative diffusivity. In the simulations discussed here, the effective value of ζ is somewhat larger than unity in most of the lower two-thirds of the box.

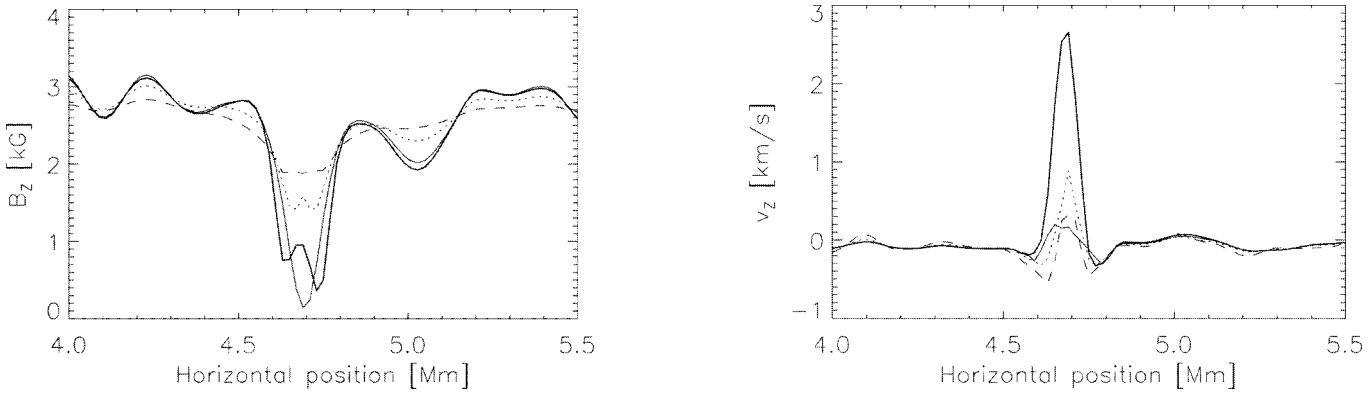

FIG. 4.—Profiles of the vertical magnetic field (*left*) and velocity (*right*) components along the horizontal direction in the cut shown in Fig. 2. In both panels, the thick solid line corresponds to constant geometric height $z = 1200$ km, and the other three lines indicate levels of constant (Rosseland) optical depth τ_R of 1 (*thin solid line*), 0.1 (*dotted line*), and 0.01 (*dashed line*). While the variation between the quantities inside and outside the upflow plume (umbral dot) is very large at the same geometric level, it is strongly reduced at equal optical depth.

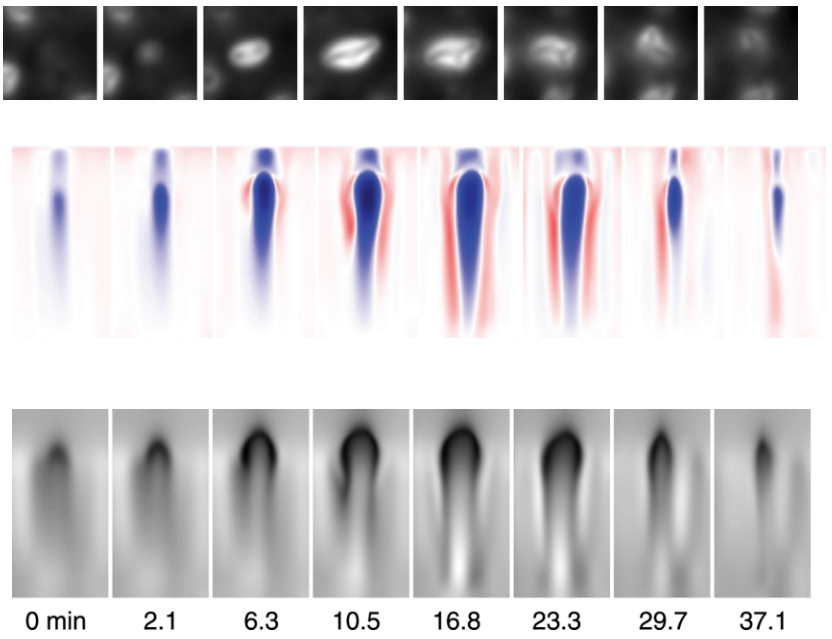

FIG. 5.—Time evolution of an upflow plume developing into an umbral dot. The panels show, from left to right, the development of the brightness (*top row*) and of vertical cuts roughly along the dark lane in the brightness images. Shown are the vertical velocity (*middle row*: *blue*, upflow; *red*, downflow) and the vertical magnetic field (*bottom row*), the cuts covering the full depth of the simulation box and 820 km in horizontal direction. The color and gray-scale schemes are the same as in Fig. 1, albeit with different ranges: $I/\langle I\rangle = 0.7$–2.25, $v_z = -1.2$ to 4.1 km s^{-1}, $B_z = -0.3$ to 3.8 kG. The snapshots are taken at the times (in minutes, relative to the first snapshot) indicated below the bottom panel. The umbral dot is clearly detectable as a bright structure for at least 25 minutes.

created by the flow, so that no significant cross-field motion is involved. Extended calculations in two dimensions have shown that (1) the character of the magnetoconvective pattern and energy transport as described above is unaffected if we halve the magnetic diffusivity, so that the results can be considered to be robust in that sense, and (2) for a run with a 4 times larger value of η, the magnetoconvection is dominated by an overturning mode with slowly evolving broad cells and cross-field flow, similar to what is predicted by linear analysis.

Our simulations reproduce the general properties of a sunspot umbra with umbral dots. The bright features resulting from the upflow plumes can be identified with (central) umbral dots; their brightness, size, and lifetime correspond well to the observations (e.g., Socas-Navarro et al. 2004). The large velocities and small field strengths in the upflow plumes are effectively hidden from spectroscopic observations by the pileup of plasma in the upper layers of the plumes, raising the formation heights of spectral lines to layers located largely above the plume. A similar underlying geometry of umbral dots has been suggested by Degenhardt & Lites (1993); their assumption of a stationary, unidirectional vertical flow is not supported by our simulation results, however.

The results show that no intrusion of field-free plasma from the underlying convection zone into a cluster-type shallow sunspot is required to explain the existence of umbral dots. In fact, a simulation with about a 15% larger value of the internal energy of the inflows resulted in flux separation, that is, the formation of large field-free patches with granule-like convection surrounded by very strong, largely homogeneous magnetic field (cf. Weiss et al. 2002), a configuration very much different from that of an undisturbed inner umbra. Therefore, a hypothetical fragmentation of the magnetic field into a cluster of flux strands has to occur at a level significantly below our bottom boundary (located ~1.6 Mm below the solar surface). However, such intrusions on a larger scale could possibly be relevant for the formation of light bridges, as well as for peripheral umbral dots connected to bright penumbral filaments.

We also ran a simulation with a field of 3500 G and the original value of the internal energy carried by the inflows. In this case, umbral dots very rarely occur and the average energy output (per unit area) is reduced to only ~9% of its value in the quiet Sun. This simulation might represent the observed dark cores of sunspot umbrae, which are largely devoid of umbral dots.

REFERENCES

Biermann, L. 1941, Vierteljahresschr. Astron. Ges., 76, 194
Choudhuri, A. R. 1986, ApJ, 302, 809
Cowling, T. G. 1953, in The Sun, ed. G. P. Kuiper (Chicago: Univ. Chicago Press), 532
Degenhardt, D., & Lites, B. W. 1993, ApJ, 404, 383
Deinzer, W. 1965, ApJ, 141, 548
Meyer, F., Schmidt, H. U., Weiss, N. O., & Wilson, P. R. 1974, MNRAS, 169, 35
Parker, E. N. 1979, ApJ, 234, 333
Savage, B. D. 1969, ApJ, 156, 707
Schlüter, A. & Temesváry, S. 1958, in IAU Symp. 6, Electromagnetic Phenomena in Cosmical Physics, ed. B. Lehnert (Cambridge: Cambridge Univ. Press), 263
Sobotka, M., & Hanslmeier, A. 2005, A&A, 442, 323
Socas-Navarro, H., Martínez Pillet, V., Sobotka, M., & Vázquez, M. 2004, ApJ, 614, 448
Spruit, H. C., & Scharmer, G. B. 2006, A&A, 447, 343
Vögler, A. 2003, Ph.D. thesis, Univ. Göttingen
Vögler, A., Shelyag, S., Schüssler, M., Cattaneo, F., Emonet, T., & Linde, T. 2003, in IAU Symp. 210, Modelling of Stellar Atmospheres, ed. N. E. Piskunov, W. W. Weiss, & D. F. Gray (San Francisco: ASP), 157
———. 2005, A&A, 429, 335
Weiss, N. O., Brownjohn, D. P., Hurlburt, N. E., & Proctor, M. R. E. 1990, MNRAS, 245, 434
Weiss, N. O., Brownjohn, D. P., Matthews, P. C., & Proctor, M. R. E. 1996, MNRAS, 283, 1153
Weiss, N. O., Proctor, M. R. E., & Brownjohn, D. P. 2002, MNRAS, 337, 293